Research Article

Nuclear-optical converters for detecting intense neutron fields[*]

Pyotr B. Baskov[1], Gleb V. Marichev[2], Vyacheslav V. Sakharov[1], Vladimir A. Stepanov[2,3]

1 All-Russian Research Institute of Chemical Technology, 33 Kashirskoye shosse, 115409 Moscow, Russia

2 Obninsk Institute for Nuclear Power Engineering, MEPhI , 1 Studgorodok, 249040 Obninsk, Kaluga Reg., Russia

3 FGBUN Interdepartmental Center for Analytical Research in the Field of Physics, Chemistry and Biology under the Presidium of the Russian Academy of Sciences, 65 Profsoyuznaya St., bldg. 6. 5117997 Moscow, Russia

Corresponding author: Vladimir A. Stepanov (stepanov@iate.obninsk.ru)

Abstract

In the design of nuclear-optical converters (NOC) for detecting intense neutron fields (fluxes over 10^{15} cm^{-2}·s^{-1}), it is proposed to use hybrid gas ionization chambers (IC), in which electrical and opticalneutron detecting methods are combined. For hybrid ICs, a technology is proposed for obtaining radiation-resistant and mechanically strong radiator materials capable of operating at temperatures of up to 1000 °C. This technology is based on solid-phase boron diffusion saturation of steel. It is shown that, at thermal neutron fluxes of 1×10^{10} n/(cm^2·s) and higher, the integral intensity of argon luminescence as a result of ionization by α-particles and ^{7}Li ions from layers of boride phases is sufficient for detection.

The combination of optical and radiation properties of multicomponent fluoride glasses makes it possible to use them as condensed active substances of NOCs. Choosing the elemental and isotopic composition, it becomes possible to use fluoride glasses for multichannel neutron detection as well as to significantly simplify the procedure for separating gamma and neutron components of radiation under conditions of intense radiation fluxes. It has been experimentally shown that in irradiation with a neutron flux of 1×10^{17} n/(cm^2·s), the intensity of Nd IR luminescence in glasses based on zirconium fluoride (ZBLAN) increases in the presence of Gd, which interacts with neutrons.

Keywords

Neutron detectors, gamma detectors, nuclear-optical converter, ionization chamber, scintillator, fluoride glass, intense neutron field

Introduction

The need to improve the existing and build new neutron detectors is explained by the changing conditions of operation for radiation devices. Thus, temperatures of up to 700 °C, neutron fluxes of up to 1×10^{17} cm^{-2}·s^{-1}, gamma dose rates of up to 1×10^2 Gy/s and vibrations of up to 200 Hz are already reached in the reactor core. Providing neutron diagnostics in reactors with such characteristics requires extending the capabilities of neutron detectors based on an electrical principle of operation via combinations with radiation luminescent detection or by switching altogether to radiation photonics systems. As small noise as possible can be achieved in radiation photonics sys-

tems under high temperature while persevering proportional detection of high-rate radiation fluxes.

Evolution of neutron detection optics is associated with the development of the nuclear-optical converter (NOC) intended to provide an autonomous neutron monitoring channel. The NOC has the following key functional components:

- a radiator of a material with components that convert the neutron flux to a flux of high-energy nuclear reaction products;
- a working medium in which high-energy ions cause excitations with the subsequent relaxation and emission of a photon flux (a mixture of inert gases or condensed scintillators);
- a fiber-optic translator that provides for the photon signal transmission to the ex-core recording equipment.

Development of each NOC component is a pending issue. Alternate solutions for the structural micro- and nanoscale arrangement of the NOC fiber-optic translators with the required operating strength under extreme external impacts can be found in (Sakharov et al. 2011, 2016). This paper considers approaches to the selection and production of radiators for hybrid ionization chambers (HIC) that combine electrical and optical methods for neutron detection, as well as approaches to selecting condensed fluids for detectors with the required sensitivity and selectivity of detection in high neutron fields (fluxes of over 1×10^{15} cm$^{-2} \cdot$s^{-1}). With regard for the specific applications of radiators and the detector working materials, a fundamental development issue is to increase the longevity via radiation resistance, mechanical strength and optical transparency in conditions of high-flux irradiation.

Hybrid chambers

Neutron diagnostics in current control and protection systems of the reactors in operation is based on ^{3}He counter tubes and ICs using ^{235}U, ^{232}Th and ^{10}B isotopes, the principle of action for which was developed as long ago as in the 1970s. An IC is a gas-filled pressure vessel with two electrodes to which an electrical potential difference is applied. Materials containing neutron-interacting isotopes are used as the IC radiator. Reactions with neutrons result in the working gas ionization by nuclear transformation products, and the ionization charge gets on the chamber's electrodes and is transmitted to the external electric circuit (Malyshev et al. 1991).

A detection system, based on radiation photonics technologies but using common fission chambers for detection, is developed in a hybrid chamber (Baskov et al. 2019). A diagram of a hybrid neutron and gamma flux detection system is presented in Fig. 1.

Apart from electrical signals from a traditional IC, such system detects the working gas bursts and glows which accompany nuclear reactions, this improving the reliability of detection and extends the neutron flux de-
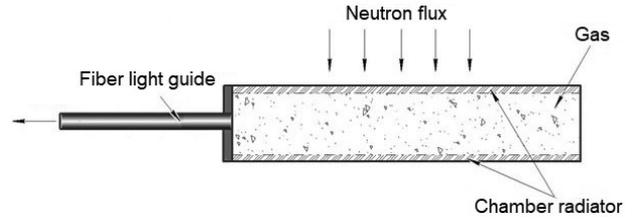

Figure 1. A diagram of a hybrid fission chamber based on single- and multicomponent radiators (^{235}U, ^{238}U, ^{232}Th, ^{6}Li, ^{10}B and other oxides) with a fiber-optic radiation-proof photon signal output.

tection range. An optic fiber is used as the channel for transmission of optical signals from the fission chamber working gas scintillations. The problem of the radiation and temperature stability of the functional components and these to be joined into a single sensitive element needs to be addressed in the hybrid fission chamber. The problem of the thermomechanical stability of radiators is resolved by forming a stable boron-containing coating on stainless steel.

Natural boron consists of two stable isotopes: ^{10}B (19.57%) and ^{11}B (80.43%). The characteristics of the stable boron isotope interaction with thermal neutrons are presented in Table 1.

Table 1. Characteristics of the stable boron isotope interaction with thermal neutrons (Potapov 1961)

Isotope	% of content in natural material	(n,α)-reaction cross-section with 0.025 eV,barn	(n,γ)-reaction cross-section with 0.025 eV, barn	Reaction of interaction with neutrons
^{10}B	19.57	3840	0.5	1) ^{10}B(n,α) → Li^{7*}+ α+2.31 2) ^{10}B(n, α) → Li^7+ α+2.79 3) ^{10}B(n,γ) → ^{11}B
^{11}B	80.43	0.005	50·10^{-3}	^{11}B(n,γ) → ^{12}B ($T_{1/2}$ = 0.019 s)

Unlike uranium, thorium and lithium isotopes used in radiators, boron, along with a large thermal neutron absorption cross-section, forms highly radiation- and heat-resistant compounds. Surface boration, e.g. for iron, cast iron and steel, is known to lead to coatings with formation of iron borides with a high surface hardness, wear resistance, heat resistance and corrosion stability (Samsonov et al. 1975). A process for diffusive boron saturation of the metal surface with formation of iron borides (Fe$_2$B and FeB) can be used to develop the IC radiators. The process is run in a mixture of boron-containing powders, pastes and gases and in molten salts (Voroshin 1981, Yevdokimov et al. 2006).

Stainless steel was selected in this study as the basis for saturating the 84% B$_4$C+16% Na$_2$B$_4$O$_7$ paste and the BF-4 glue in acetone. The saturation took place at 1000 °C with a protective layer composed of 50%B$_2$O$_3$+50%SiO$_2$. It was shown using an X-ray phase analysis that such chemicothermal treatment leads to a solid layer of Fe$_2$B and FeB borides formed on the surface. The microstructure of the radiator sample section is shown in Fig. 2. There is
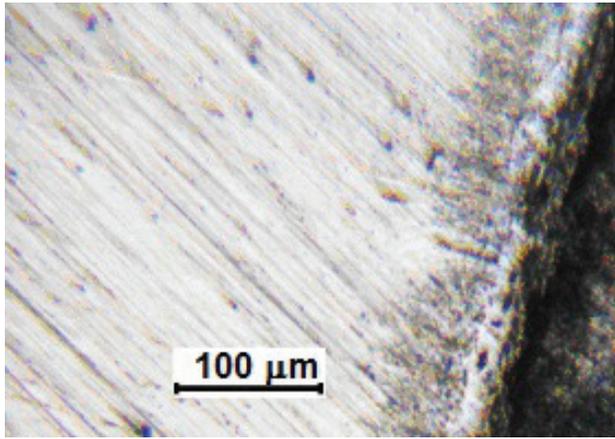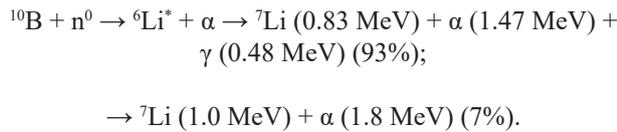
Figure 2. Sample section microstructure of a radiator of stainless steel following the boration process.

a boride layer with a depth of up to 50 μm visible on the surface. The microhardness of the layer was 9.1 GPa as compared with the initial value of 2.2 GPa for steel.

To estimate the efficiency of such radiator, we shall assume that, as shown in Table 1, lithium and helium ions escape from the radiator surface as the result of the following reactions:

$$^{10}B + n^0 \rightarrow {}^6Li^* + \alpha \rightarrow {}^7Li \ (0.83 \ MeV) + \alpha \ (1.47 \ MeV) + \gamma \ (0.48 \ MeV) \ (93\%);$$

$$\rightarrow {}^7Li \ (1.0 \ MeV) + \alpha \ (1.8 \ MeV) \ (7\%).$$

The ion fraction, $f(x)$, escaping into the gas from depth x from the electrode surface is

$$f(x) = 1/[2(1 - x/R)],$$

and the overall fraction of the ions escaping into the gas is obtained with coating thickness s being larger than ion range R

$$f = \frac{\int_0^R f(x)dx}{s} = \frac{R}{4s}.$$

The results of calculating the He and Li ion fluxes from borated steel layers are shown in Table 2.

Table 2. Results of calculating ion fluxes from boride phases

Phase	ρ, g/cm^3	Neutron absorption factor, cm^{-1}	α (1.47 MeV)			^{7}Li (0.87 MeV)		
			Range R, μm	f	Flux q, 10^{10} ion/(cm^{2}s)	Range R, μm	f	Flux q, 10^{10} ion/(cm^{2}s)
FeB	5.1080	34.64	2.96	0.1850	6.41	1.82	0.1138	3.94
Fe2B	6.0273	22.24	2.71	0.1694	3.77	1.39	0.0869	1.93

Argon suits best for the hybrid chamber working medium. This is explained by the fact that the arc and spark spectra of argon consist of many lines (about 900) situated in the spectral region between 400 and 706 nm (Striganov and Sventitsky 1966, Physical Quantities: Handbook 1991). According to (Omarov et al. 2013), the emission

spectrum of the argon spark discharge is characterized by intensive line and recombination radiation with a burst length of up to 1×10^{-8} in a wavelength range of 200 to 600 nm. The argon luminescence falls within the transparency range in the red and near-IR region of fiber-optic quartz translators even with high radiation impacts. Estimates for the hybrid chamber luminescence during thermal neutron irradiation, with regard for the argon energy conversion efficiency of 0.03, are presented in Table 3.

Table 3. Results of calculating the luminous intensity of the hybrid chamber argon during thermal neutron irradiation of 1×10^{10} n/cm^{2}s

Ion	FeB			Fe2B		
	Eav, MeV	Ion energy flux, 10^{10} MeV/(cm^{2}s)	Luminous intensity I, mW/cm^2	Eav, MeV	Ion energy flux, 10^{10} MeV/(cm^{2}s)	Luminous intensity I, mW/cm^2
α	0.818	5.243	0.251	0.752	2.835	0.136
^{7}Li	0.492	1.938	0.093	0.195	0.376	0.018

The full solid angle luminous intensity will be up to 0.3 mW. Even with the inevitable loss in the course of the radiation fiber interception in the hybrid chamber, such intensity will allow confident neutron flux detection starting with 1×10^{10} n/cm^{2}s.

Multicomponent glasses

Condensed oscillators have long been used as the NOC working medium (Yegorov 1963). Unlike gas that is insensitive to gamma radiation, solid-body detectors based on inorganic crystals, glasses and organic plastic scintillators can be used to detect both neutrons and gamma quanta. Ionization by gamma radiation takes place as result of a photoelectric effect for quanta energies of below 0.5 MeV, Compton scatter or creation of electron-positron pairs for energies of over 1 MeV. Interaction of neutrons involves either ion knocking out or nuclear reactions the products of which also ionize the medium.

Table 4 presents characteristics of the most common scintillators. High-density materials (inorganic NaI, CsI, BGO and other crystals) are used predominantly for greater absorption in detection of gamma radiation). Organic water-containing scintillators, e.g. anthracene and

Table 4. Characteristics of selected materials used in scintillation counters

Material	Density, g/cm^3	Luminescence time, 10^{-9} s	Wavelength in spectrum maximum, nm	Energy conversion efficiency, % (for electrons)
Anthracene, $C_{14}H_{10}$	1.25	30	445	4
Stilbene, $C_{14}H_{12}$	1.16	6	410	3
NaI (Tl)	3.67	250	410	6
ZnS (Ag)	4.09	11	450	10
CsI (Tl)	4.5	700	560	2
CaF$_2$(Eu)	3.18	940	435	3
Bi$_4$Ge$_3$O$_{12}$	7.13	350	480	0.6
CdWO$_4$	7.90	1000	530	1.2
Glass, SiO$_2$(Ce)-Li	2.2	200	480	5
HBLAN (Ce)	6	25	320	~1

stilbene, in which the protons knocked out by neutrons ionize the medium, are used for neutron detection. Thermal neutrons are absorbed in lithium-containing quartz glass by interactions with the ^{6}Li isotope. Energetic alpha particles and tritium are formed which ionize the medium and excite the Ce^{3+} scintillation impurity (Patent USA 5680423). Glasses based on metal fluorides may serve as detectors of both gamma quanta (due to their high density) and neutrons (thanks to a high cross-section of the neutron capture by the nuclei contained in elements). For instance, glasses with hafnium fluoride and a cerium impurity (HBLAN in Table 4) with a reasonably good energy conversion efficiency were proposed for detection of X-ray and gamma radiation in 1996 (Hobson et al. 1996).

With gamma radiation and neutron components being simultaneously detected, the optical scintillations caused by neutrons and gamma quanta are separated as the result of processing statistically the amplitudes and time responses of individual scintillations. They differ during the interactions of gamma quanta and neutrons with the material (Yegorov 1963). The most important characteristics of the detector materials are therefore the energy conversion efficiency, i.e. the ratio of the light energy to the absorbed radiation energy, as well as the luminescence time on which the material ionization pulse distortion degree depends.

Such detection method often leads to major uncertainties, specifically in high neutron fields with fluxes of over 1×10^{15} cm$^{-2} \cdot$s^{-1}. First, to implement a statistical analysis of scintillations, representative luminescence times shall not exceed a few to tens of nanoseconds to avoid the signal interferences. However, individual, even short oscillations coalesce to form a solid background in high radiation fields, this making it completely impossible to investigate their shape and duration. Second, short scintillations of optically active impurities in materials turn out to be in visible and ultraviolet bands, in which major optical degradation of the materials as such takes place with the growth in the radiation exposure dose (Stepanov et al. 2002).

The above issues are coped with by using multicomponent glasses and by giving up the method of counting and analyzing individual scintillations from radiation fluxes (Baskov et al. 2015). For example, fluoride glasses permit broad variations of the elemental composition in terms of components interacting with neutrons and luminescent admixtures. This makes it possible to use them for simultaneous detection of gamma quanta and neutrons by measuring and comparing integral luminous intensities. It also enables optical measurements in the IR region by selecting the luminescent admixture for reducing the radiation-induced optical losses and switching to detection of high fluxes.

Glasses based on hafnium and zirconium fluorides were studied for using fluoride glasses as the NOC working medium (Sakharov et al. 2004):

HBLAN – 54%HfF$_4$24%BaF$_2$3%AlF$_3$18%NaF1%InF$_3$,
ZBLAN – 52%ZrF$_4$20%BaF$_2$4%LaF$_3$4%AlF$_3$20%NaF.

Nuclei of hafnium and zirconium elements differ greatly in terms of the neutron interaction cross-section but glasses based on these have similar optical properties. Fig. 3 shows gamma radiation absorption spectra for the most common NaI detector and the fluoride glass spectra we have calculated. Glasses in the most interesting region of about 1 MeV prove to be not worse and hafnium glass even better than NaI crystals in terms of gamma radiation absorption.
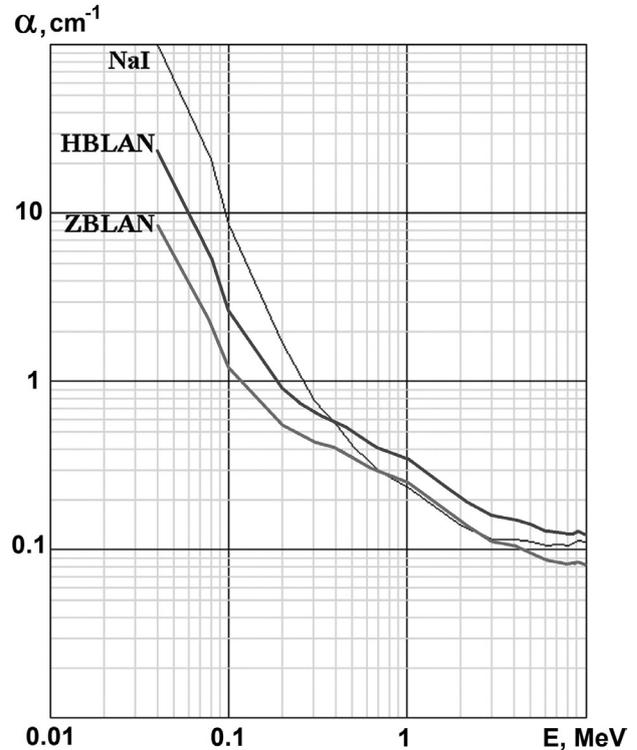
Figure 3. Gamma radiation absorption spectra for detector materials.

With ionizing irradiation, fluoride glasses luminesce in the UV and visible spectrum ranges (Fig. 4) without scintillation admixtures (Baskov et al. 2002a). Spectra of fluoride
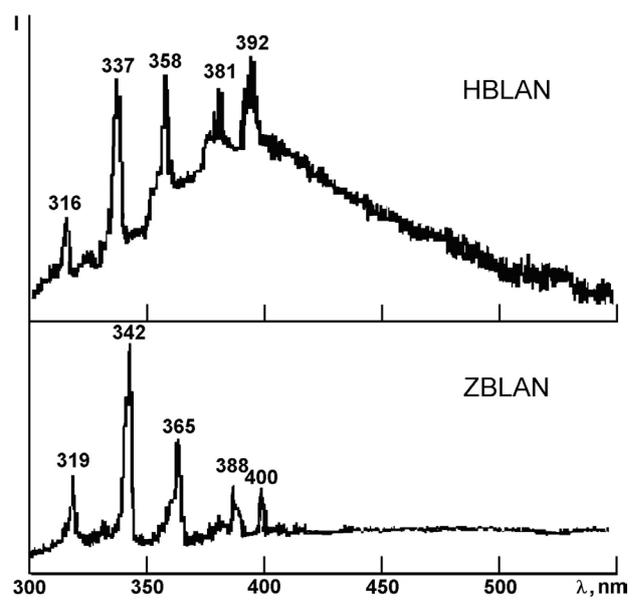
Figure 4. Luminescence spectra for glasses based on hafnium fluoride (HBLAN) and zirconium fluoride (ZBLAN) in the process of irradiation with protons of 8 MeV.

glasses are characterized by a series of narrow lines in a range of 300 to 400 nm. Such lines in the UV spectrum range are associated with core-and-valence flash luminescence and cross luminescence. The cross luminescence mechanism consists in that the knocking-out of electrons from the internal levels leads to the transitions from the valence band to the vacant spaces in the internal core shells being accompanied by the emission of light rather than by Auge yield (Makhov et al. 1995). In terms of intensity, cross luminescence of fluoride glasses is much smaller than impurity luminescence but takes place at times of up to 50 ns and does not depend on the radiation dose of up to 1 MGy.

Fluoride glasses in conditions of radiation effects are transparent in a broader wavelength range than crystals and glasses based otherwise. Irradiated fluoride glasses restore their optical properties in the process of photoelectric annealing. Photoelectric restoration of the optical properties of gamma irradiated fluoride glasses is effective with light intensities of just 1 mW/cm² (Baskov et al. 2002b).

Isotopes with a high (n, α) reaction cross-section (^{6}Li, ^{10}B) or a high probability of the (n, γ) radiative capture reaction (Hf, Cd, Gd, ,I and others) may be chosen when selecting the elemental composition for detection of radiation fluxes as interacting with neutrons of the glass components. Radiative capture involves nearly instantaneous liberation of energy of about 7.5 MeV in the form of gamma radiation that is absorbed and ionizes the glass. Fig. 5 shows dependences of the neutron cross-sections for Zr, Hf and Gd nuclei. It can be seen that the differences in the cross-sections reach several orders of magnitude. Therefore, when comparing radiation-induced luminescence for different glasses containing such elements, one can estimate the quantity of thermal, intermediate and even fast neutrons in the radiation flux. This also enables multichannel detection in which n- and γ-components of radiation are separated by way of comparing the integral intensities of luminescence for glasses with different compositions.

Fig. 6 presents luminous spectra for ZBLAN glasses with Nd impurity in conditions of pulsed reactor radiation (a pulse of 80 μs, a dose of 5×10¹² neutron/cm² (E > 1
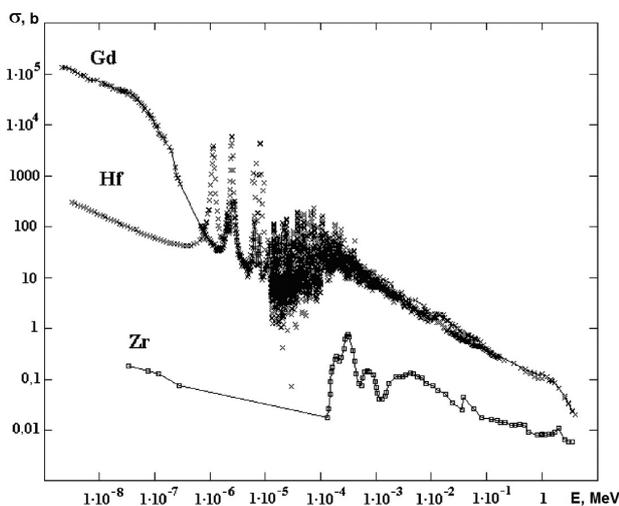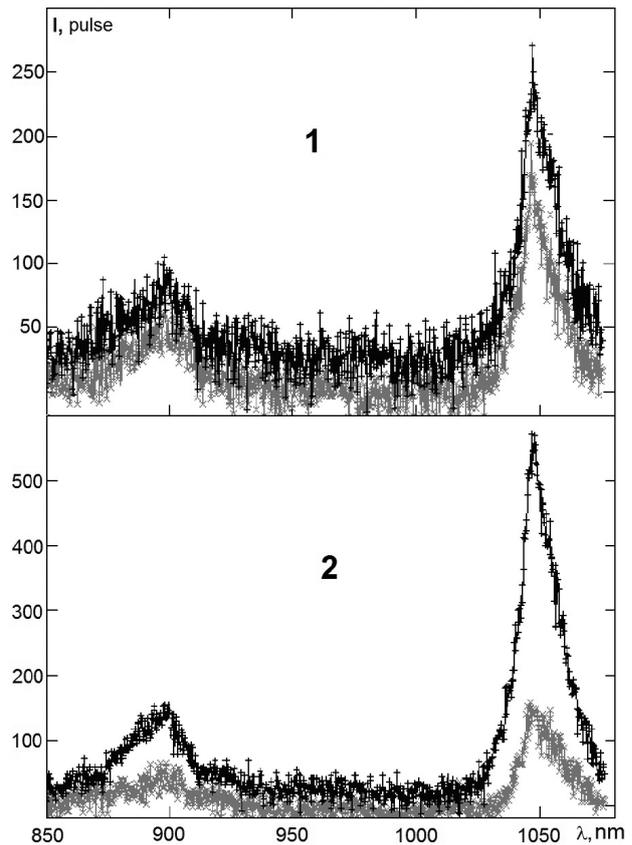

Figure 6. Spectra of optical signals in glasses: ZBLAN(Nd) (grey) and ZBLAN(Nd,Gd) (black), with pulsed reactor irradiation: 1 – fast spectrum; 2 – degraded neutron spectrum.

keV) per pulse, a gamma quanta dose of 9 Gy). An impurity with a high cross-section of interaction with neutrons (Gd) was introduced into one of the glasses. The optical signal transmission from the glasses was through radiation-resistant KU-1 fibers. Measurements were done with the NOC components being in the immediate vicinity of the reactor cores, as well as in a polyethylene tank for the neutron spectrum degradation.

The NOC luminescence spectra are the Nd luminous spectra with a band with the maximum of 900 nm and a narrow line at 1050 nm. The luminescence from the ZBLAN(Nd) element is associated only with the reactor gamma radiation. The neutron component of the radiation field is another contributor to the ZBLAN(Nd,Gd) luminous intensity. This is clearly seen when comparing the luminous intensity of glasses with and without Gd, as well as during irradiation with fast and thermal neutrons for which the Gd (n,γ) reaction cross-section differs by several orders of magnitude (see Fig. 5). The neutron spectrum degradation leads to an increased luminous intensity of only the ZBLAN(Nd,Gd) element, while the ZBLAN(Nd) luminescence does not change.

Conclusion

Hybrid gas ICs, which combine electrical and optical methods of neutron detection, are proposed in developing a NOC for detection of high neutron fields

Figure 5. Cross-sections of the neutron capture reactions for elements as a function of neutron energy (McLane 2000).

(fluxes of over 1×10^{15} cm^{-2}·s^{-1}). A technology for producing radiation-resistant radiator materials fit for service at temperatures of up to 1000 °C is proposed for hybrid ICs. Solid-phase diffusive boron saturation of 12Kh18N10T steel makes it possible to produce IC radiators with FeB and Fe$_2$B phase layers with a thickness of up to 50 μm and a microhardness of up to 9.1 GPa. It has been shown that with a thermal neutron flux of 1×10^{10} n/cm^2·s, the integral luminous intensity of argon from ionization with alpha particles and ^{7}Li ions is 0.35 mW/cm^2 from FeB phase layers and 0.15 mW/cm^2 from Fe$_2$B phase layers.

Combining the optical and radiation properties of multicomponent fluoride glasses enables their use as the condensed NOC working media and in integral neutron and gamma flux detectors. Major variations of the elemental and isotope compositions can be used to increase the sensitivity to the neutron and gamma components of high-rate radiation fluxes and optimize the energy conversion efficiency of glasses. It has been shown experimentally that the luminous intensity of Nd (900 and 1050 nm) in ZBLAN glasses with the addition of a Gd impurity, which is active to neutrons, increases during neutron irradiation of 1×10^{17} n/(cm^2·s) and gamma quanta irradiation of 1×10^5 Gy/s. The neutron spectrum degradation leads to an increased luminous intensity of the ZBLAN glass with Gd thanks to an increased cross-section of interaction with neutrons.

References

■ Baskov PB, Kurdyavko PV, Plaksin OA, Sakharov VV, Stepanov VA, Stepanov PA (2002a) Radio-luminescence of fluoride glasses. Proc. of the 13th Int. Symposium on Non-Oxide Glasses and New Optical Glasses. Pardubice, Czech Republic, Part II, 534–536.

■ Baskov PB, Marichev GV, Sakharov VV, Stepanov VA (2019) Hybrid chambers for detection of neutron fields. Proc. of the 14th All-Russian Scientific Conference on Technologies and Materials for Extreme Conditions, ed. Acad. B.F. Myasoyedov. MTsAI RAN Publ., Moscow, 332–336. [in Russian]

■ Baskov PB, Sakharov VV, Stepanov VA (2015) Multicomponent fluoride glasses for detection of radiation fields. Voprosy radiatsionnoy bezopasnosti 3: 115–120. [in Russian]

■ Baskov PB, Sakharov VV, Stepanov VA, Stepanov PA, Kurdyavko PV (2002b) Photoinduced recovery of gamma-irradiated fluoride glasses. Technical Physics Letters 28(9): 790–791. https://doi.org/10.1134/1.1511787

■ Hobson PR, Imrie DC, Price T, Bell KW, Brown RM, Cockerill DJA, Flower PS, Grayer GH, Lintern AL, Sproston M, McKinlay KJ, Parker JM (1996) Dense, fast, radiation-tolerant fluoro-hafnate glass scintillators for electromagnetic calorimeters in high energy physics. Proc. of the Int. Conf. on Inorganic Scintillators and Their Applications (SCINT95). Delft University Press, Netherlands, 317–324.

■ Makhov VN, Kamenskikh IA, Terekhin MA, Munro IH, Mythen C and Shaw DA (1995) Effect of quenching processes on decay of fast luminescence from BaF$_2$ Proc. of the Int. Conf. on Inorganic Scintillators and Their Application (SCINT95), 208–211.

■ Malyshev YeK, Zasadych YuB, Stabrovsky SA (1991) Gas Discharge Detectors for Monitoring of Nuclear Reactors. Moscow. Energoatomizdat Publ., 160 pp. [in Russian]

■ McLane V (2000) EXFOR Basis. A Short Guide to the Nuclear Reaction Data Exchange Format. BNL-NCS/05-Rev. https://doi.org/10.2172/767143

■ Omarov OA, Omarova NO, Omarova PKh, Ramazanova AA, Al-Khareti FMA, Khachalov MB (2013) Plasma spectroscopy for the spark breakdown of gases in strong magnetic fields. Inzhenernaya fiizika 5: 50–58. [in Russian]

■ Patent USA 5680423 (Oct.1997) Perkins, et al. (class USA 376/153).

■ Physical Quantities: Handbook (1991) Physical Quantities: Handbook. Grigoryeva IS, Meylikhova YeZ (Eds). Energoatomizdat Publ., Moscow, 1232 pp. [in Russian]

■ Potapov SP (1961) On the Use of Stable Boron Isotopes. Atomnaya energiya 10(3): 244–252. [in Russian]

■ Sakharov VV, Baskov PB, Berikashvili VSh, Ivkina OV, Kosov DYe, Mosyagina IV, Frolov NN, Sharipova MA (2011) An oxide nanoscale modification of the surface of inorganic materials. Nanoinzheneriya 6: 15–25. [in Russian]

■ Sakharov VV, Baskov PB, Stepanov VA, Stepanov PA, Federov VD (2004) Oxygen-free optical materials for radiation optics. VANT. Ser. Materialovedeniye i novyye materialy 1(62): 231–244. [in Russian]

■ Sakharov VV, Mosyagina IV, Baskov PB, Stepanov VA (2016) Combinatorics of physics and materials research for film and fiberglass materials for radiation-luminescent detection of neutron fluxes. Voprosy radiatsionnoy bezopasnosti 2(82): 55–63. [in Russian]

■ Samsonov GV, Serebryakova TI, Neronov VA (1975) Borides. Atomizdat Publ., Moscow, 376 pp. [in Russian]

■ Stepanov VA, Baskov PB, Chernov VM, Fedorov VD, Khorozova OD, Kurdyavko PV, Sakharov VV, Stepanov PA (2002) Fluoride glasses as materials for radiation optics. Proc. of the 13th Int. Symposium on Non-Oxide Glasses and New Optical Glasses. Pardubice, Czech Republic, Part II, 674–677.

■ Striganov AR, Sventitsky NS (1966) Tables of Spectral Lines. Atomizdat Publ., Moscow, 900 pp. [in Russian]

■ Voroshin L (1981) Boration of Industrial Steels and Cast Irons: Reference Book. Belarus Publ., Minsk, 205 pp. [in Russian]

■ Yegorov YuA (1963) Scintillation Method for Spectrometry of Gamma Radiation and Fast Neutrons. Gosatomizdat Publ., Moscow, 306 pp. [in Russian]

■ Yevdokimov VD, Klimenko LP, Yevdokimova AN (2006) Hardening Technology for Machine-Building Ma terials: Training Reference Book. 2nd ed. Professional Publ., Kiev, 352 pp. [in Russian]